Bangladesh J. Bot. **55**(1): 191-199, 2026 (March) DOI: https://doi.org/10.3329/bjb.v55i1.88762

10-M MAPPING AND ANALYSIS OF MAJOR CROP PLANTING PATTERNS IN HENAN PROVINCE IN CHINA

YING FANG, HANG LIU[1], YUZHU LIU[2,3], RUI CHENG[4,5]* AND JINQIU ZOU[6*]

School of Information Technology, Shangqiu Normal University, Shangqiu Henan 476000, China

Keywords: XGBoost Algorithm, Crop planting systems, Remote sensing, Henan Province, Food security, SHAP

Abstract

To improve crop mapping in complex agricultural regions for food security, this study develops a seasonal monitoring framework, treating the growing seasons as independent classification tasks based on specific temporal windows, in Henan Province, China, using 2023 Sentinel imagery. It employs separate feature sets for summer-harvested (winter wheat) and autumn-harvested crops (maize, rice, peanut, soybean), using an XGBoost algorithm for classification and a SHAP model to overcome the black-box nature of the algorithm and identify key phenological markers. The framework demonstrated high effectiveness, achieving cross-validation consistency rates of 85.18% for winter wheat and 90.08% for maize. The resulting maps show that a winter wheat-summer maize rotation is the predominant cropping pattern in the province. The study also found that driving factors for classification differ by season: winter wheat identification depends on unique phenological signals (e.g., March NIR), whereas autumn crops are distinguished by a dual mechanism of macro-geographical latitude and specific spectral indices. This research confirms the strategy's robustness for fine-scale mapping.

Introduction

Ensuring national food security is a fundamental pillar of socioeconomic stability and sustainable global development (Yang e*t al*. 2020). The timely and precise mapping of crop spatial distribution and planting patterns in major grain-producing regions is essential for optimizing agricultural resource allocation and accurately assessing grain production capacity (Waha *et al.* 2020, Hu *et al*. 2025). With its advantages of broad coverage, short revisit cycles, and cost-effectiveness, remote sensing has emerged as a critical technology for rapidly acquiring large-scale information on agricultural landscapes. Significant progress has been made in using time-series satellite imagery to map the distribution of individual crops such as rice (Zhang *et al*. 2017), maize (Qiu *et al.* 2018, Jin *et al*. 2019), wheat, soybean, and rapeseed. Some studies have extended this to mapping multiple crop types (Griffiths *et al.* 2019, You *et al.* 2021).

However, research focusing on the remote sensing of entire planting patterns in regions with complex agricultural systems remains relatively scarce (Blickensdörfer *et al.* 2022, Qiu *et al.* 2022). In areas characterized by high crop diversity and intricate cropping systems, accurately distinguishing between various crop types and reconstructing their annual rotation cycles from satellite imagery presents a persistent challenge in the field of agricultural remote sensing (Wu *et al.* 2023). Previous studies attempting to map these complex systems often fall short due to the high spectral similarity among concurrent autumn crops and an insufficient temporal resolution to capture tightly linked rotation sequences (Cai *et al.* 2018, Blickensdörfer *et al.* 2022, Wu *et al.* 2023, Qi *et al.* 2024). Henan Province, as one of China's core grain production areas, plays a vital

*Author for correspondence: <caaschengrui@163.com>, <zoujinqiu@caas.cn>. [1]Dongfang College, Zhejiang University of Finance and Economics, Jiaxing 314408, China. [2]School of Public Affairs, Zhejiang University, Hangzhou 310058, China. [3]Zhejiang University Urban-Rural Planning& Designing Institute Hangzhou Zhejiang 310058, China. [4]Institute of Geographic Sciences and Natural Resources Research, Chinese Academy of Sciences, Beijing, 100101. [5]University of Chinese Academy of Sciences, Beijing, 101408, China. [6]Institute of Agricultural Resources and Regional Planning Chinese Academy of Agricultural Sciences, Beijing 100081, China.

role in Chinese food security (Wang *et al.* 2024a). Its dominant winter wheat-summer maize rotation is a representative planting pattern with tightly linked growing seasons (Yang *et al.* 2023).

This spatiotemporal heterogeneity is further exacerbated by a north-south thermal gradient that causes phenological shifts. For instance, winter wheat in southern Henan typically matures earlier than in northern regions, posing a challenge for classification models that rely on spectral information (Griffiths *et al.* 2019, Diao 2020). Previous studies in Henan have often focused on a single season, neglecting the complete summer-autumn cropping sequence and the distinct drivers of autumn crops (Tian *et al.* 2023).

To address these challenges, this study develops an interpretable seasonal monitoring framework. By integrating multi-source data, we constructed season-specific feature sets to capture critical phenological information. To ensure robustness, feature selection was performed (Burchard-Levine *et al.* 2021, Tufail *et al.* 2025), and the XGBoost (Chen *et al.* 2016) algorithm was utilized. The SHAP method was subsequently applied to interpret the classification results, moving beyond 'black-box' predictions to provide actionable insights into crop-specific spectral and phenological behaviors (Antwarg *et al.* 2021). The primary objectives are: 1) to produce high-precision (10 m) maps of crops and planting patterns in Henan for 2023 and 2) to quantitatively decode the underlying phenological and geographical drivers using SHAP values.

Materials and Methods

The study was conducted in Henan Province, a major grain-producing region in China (31°23′–36°22′N, 110°21′–116°39′E; Fig. 1). The province experiences a distinct transitional climate, ranging from a warm temperate monsoon climate in the north to a humid subtropical climate in the south (Wang *et al.* 2024b). The agricultural landscape is characterized by a complex winter wheat-summer maize double-cropping system. In 2021, winter wheat covered 5.691 million hectares (Mha), followed by major autumn crops including maize (3.867 Mha), peanut (1.318 Mha), soybean (0.364 Mha), and rice (0.602 Mha). This combination of crop diversity and spatiotemporal heterogeneity, driven by a north-south thermal gradient, provides a representative landscape to validate the proposed seasonal monitoring framework.

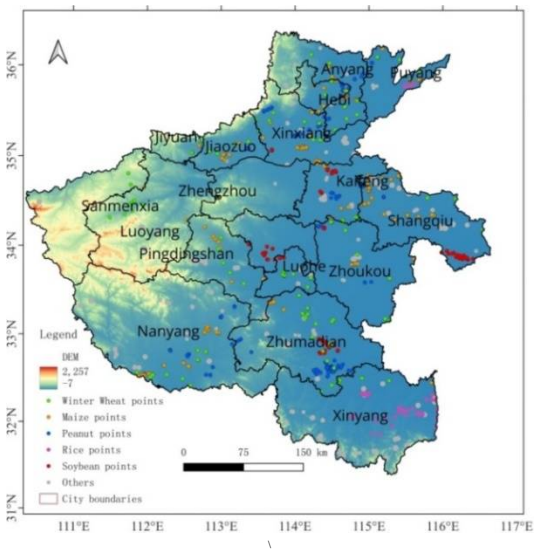

Fig. 1. Location and sample point distribution of the study area in Henan Province.

This research used a multi-source dataset for the 2023 growing seasons. Time-series Sentinel-2 L2A imagery (10 m) was processed on the GEE platform, involving cloud-masking (>50% probability) and the calculation of monthly maximum NDVI and LSWI composites to capture phenology. MODIS NDVI products, resampled to 10 m spatial resolution using bilinear interpolation to match the Sentinel-2 scale, were used for gap-filling, and Sentinel-1 SAR data (10 m, VH polarization) from July-August was included to aid rice identification by mitigating spectral confusion. Auxiliary data included a 10 m Copernicus DEM to derive slope, the 2023 GLC_FCS10 land cover product to provide spatial context, and pixel-level geographic coordinates to model spatial heterogeneity. Ground truth data were generated by creating sample points within manually digitized polygons based on 2023 sub-meter Jilin-1 base maps, Esri World Imagery, Google Earth, and Sentinel-2 multispectral imagery for each class (Table 1). For independent validation, we extracted high-confidence 'pure pixel' samples (centre pixel and 7x7 neighborhood) from third-party winter wheat and maize datasets.

Table 1. Summary of ground truth sample and validation points.

Data Category	Class	No. of polygons	No. of points
Sample points	Winter wheat	125	12500
	Maize	143	14300
	Rice	80	8000
	Peanut	155	15500
	Soybean	95	9500
Validation data	Winter wheat (Dong *et al.* 2020)	-	31103
	Maize (Peng *et al.* 2023)	-	14894

Our methodological framework employed a seasonal monitoring approach to accurately map the complex cropping systems. We developed separate feature sets tailored to the specific growing seasons: a 34-feature set for the summer season (dominated by winter wheat) and a 61-feature set for the autumn season (maize, rice, peanut, soybean), as detailed in Table 2. This feature design was based on the distinct phenological profiles of the crops; for example, winter wheat's unique spring green-up period allows clear separation from summer-sown autumn crops (Fig. 2).

Table 2. Summary of feature sets used for seasonal crop classification.

Feature category	Summer-harvested model	Autumn-harvested model
Spectral	Sentinel-2 bands (Mar, Apr: B2, B3, B4, B5, B6, B7, B8, B8A, B11, B12)	Sentinel-2 bands (Jul, Aug, Sep, Oct: B2, B3, B4, B5, B6, B7, B8, B8A, B11, B12) Sentinel-1 bands (Jul, Aug: VV, VH)
Phenological	Time-series NDVI (Sep 2022 – Jun 2023)	Time-series NDVI (May – Nov 2023) Time-series LSWI (Jun – Oct 2023)
Geographical	DEM, slope, aspect, land cover	DEM, slope, aspect, land cover, longitude, latitude
Total features	34	61

Crop classification was performed using the XGBoost algorithm (implemented via the Python xgboost library v2.1.4). The summer task was simplified to a binary classification (wheat vs non-wheat) due to winter wheat's dominance (66.61% of summer grain area). Optimal hyperparameters were determined via grid search (max_depth = 10, learning_rate = 0.1, subsample = 0.8, colsample_bytree = 0.8). We employed a two-step SHAP process to balance model efficiency and interpretability. In the first step, SHAP attribution was utilized as a feature pruning mechanism; we evaluated the global importance of all initial variables and dropped low-impact features to reduce model complexity and mitigate potential overfitting. In the second step, SHAP was applied to the refined model to interpret the final results by quantifying each feature's contribution. Finally, annual planting patterns were mapped by fusing the seasonal results. A 3-pixel morphological dilation was applied to the winter wheat parcels to create a fault-tolerant mask. This 3-pixel window was chosen to account for edge effects in small parcels and compensate for GPS inaccuracies. The mask was then overlaid with the autumn crop map to identify rotation sequences like "Winter Wheat-Summer Maize".

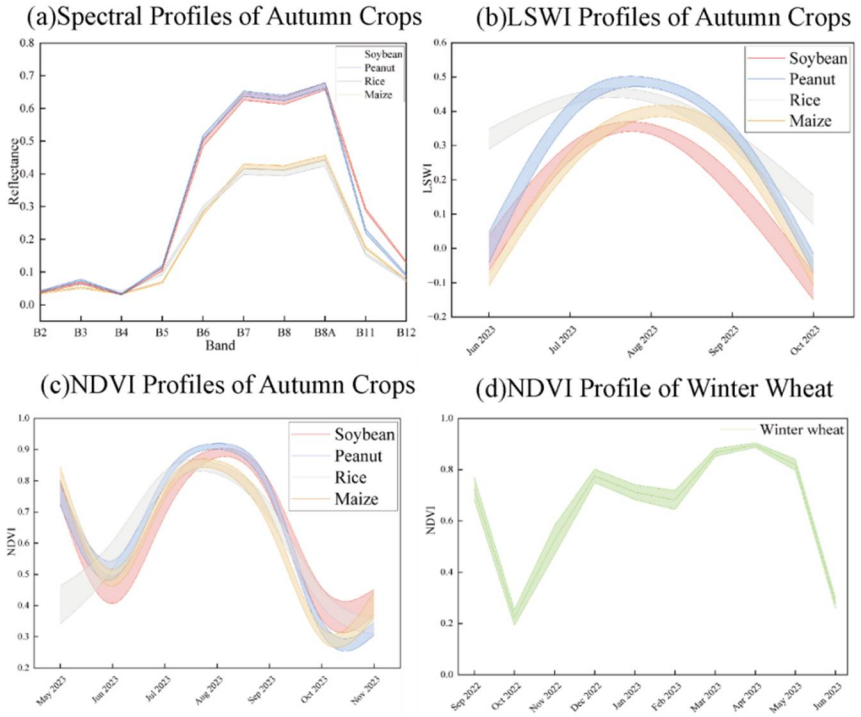

Fig. 2. Remote sensing characteristic curves of major crops in Henan Province. (a) Spectral reflectance of autumn crops in August from Sentinel-2; (b) Time-series LSWI profiles of autumn crops; (c) Time-series NDVI profiles of autumn crops; (d) Time-series NDVI profile of winter wheat.

Results and Discussion

The seasonal monitoring framework successfully extracted the spatial distributions of summer and autumn crops, producing high-precision maps of crop types (Fig. 3) and their annual rotation patterns (Fig. 4). The mapping results reveal that a winter wheat-summer maize rotation is

the most predominant planting pattern in Henan, covering an estimated 3.91 million hectares. Other significant rotations include winter wheat-peanut (0.83 Mha), winter wheat-soybean (0.49 Mha), and winter wheat-rice (0.12 Mha).

The accuracy of these maps was confirmed through a multi-level validation process. A cross-validation with independent, third-party datasets showed high reliability, with a mapping consistency of 85.18% for winter wheat and 90.08% for maize (Fig. 3). A macro-scale comparison with official statistics further validated these findings, showing good agreement for most major crops, such as a relative difference of only -3.02% for winter wheat (Fig. 4). However, this comparison also highlighted a significant overestimation of the soybean area (102.75%). This discrepancy is likely due to spectral confusion with other cash crops (e.g., sunflower and cotton), spectrally similar weeds, and other late-summer crops like mung beans. Furthermore, soybeans in Henan are frequently cultivated in small, highly fragmented plots, which exacerbates the mixed-pixel effect and inevitably leads to over-classification. Conversely, the discrepancies observed for maize (+14.49%) and peanut (-27.43%) highlight a common divergence between remote sensing and official agricultural surveys. Official statistics may under-report complex intercropped areas by categorizing the land under a single primary crop, whereas our pixel-based remote sensing approach captures the actual green cover of these respective crops. Therefore, independent cross-validation with third-party datasets provides a more conservative yet realistic estimate of model performance (Thenkabail and Aneece 2019, Maleki *et al.* 2024, Xiao *et al.* 2025).

Table 3. Cross-validation results with third-party products.

Crop type	Third-Party product	Total validation points	Consistent points	Consistency rate
Maize	CCD-Maize (Peng *et al.* 2023)	14894	13417	90.08%
Winter Wheat	China Winter Wheat Dataset (Dong *et al*. 2020)	31103	26493	85.18%

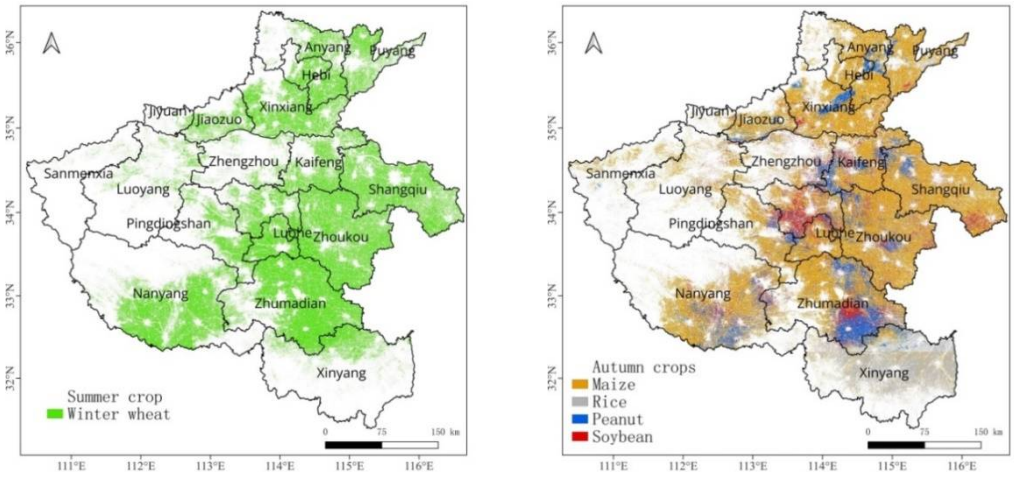

Fig. 3. Remote sensing mapping results of multiple crop types in Henan Province. (a) Summer crop: winter wheat; (b) Autumn crops: maize, rice, peanut, soybean.

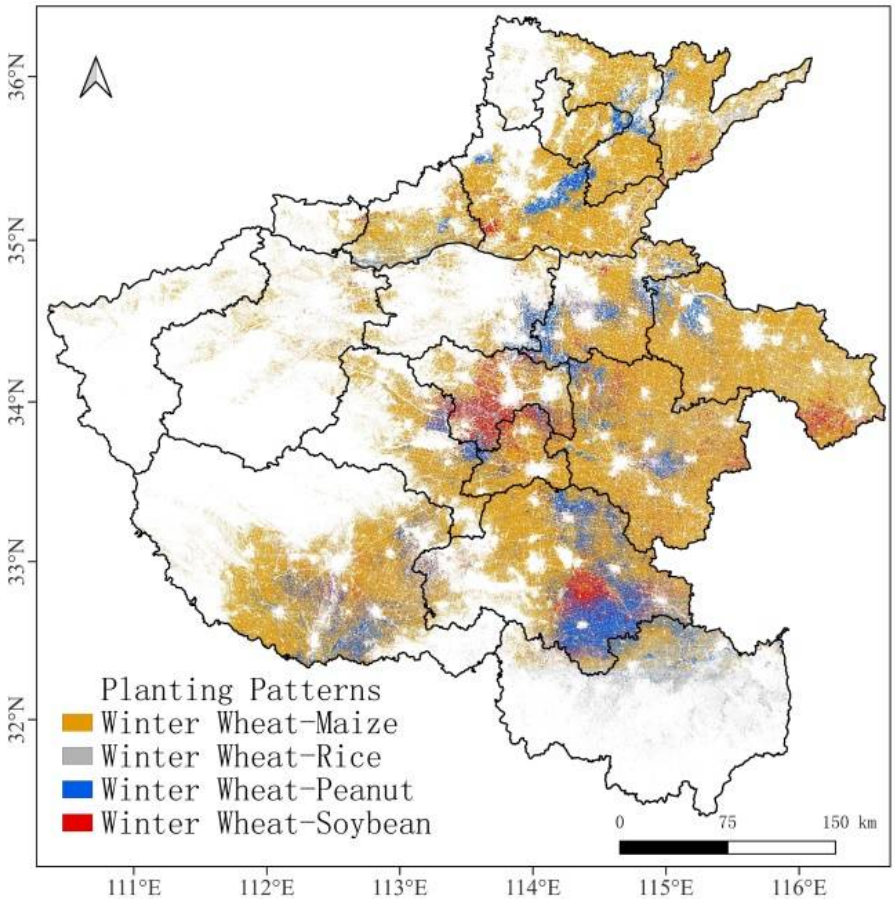

Fig. 4. The spatial distribution results of crop planting systems in Henan Province.

Table 4. Comparison of remote sensing-derived area and official statistical data.

Crop type	Mapped area (Million Hectares)	Statistical data (Million Hectares)	Relative error (%)
Winter Wheat	5.50	5.67	-3.02
Maize	4.43	3.86	14.49
Peanut	0.95	1.31	-27.43
Rice	0.58	0.60	-3.66
Soybean	0.74	0.36	102.75

To understand the drivers behind the successful classification, a SHAP analysis was performed to interpret the model's decisions. The analysis revealed that the model relied on distinct phenological and geographical features to differentiate crops. Although the external "Land Cover Type" initially ranked high as a macro-level cropland filter, we excluded this categorical

variable from the final interpretative ranking (Table 5) to prevent it from overshadowing the actual physiological insights. This allowed us to focus strictly on the spectral, phenological, and continuous geographical drivers of the crops. For winter wheat, the classification was principally driven by its unique phenological rhythm. The SHAP model identified the near-infrared (NIR) bands in March and the NDVI in December as the most critical features (Table 5), which correspond perfectly to winter wheat's key growth stages (spring green-up and pre-dormancy) and are consistent with previous findings.

In contrast, the spatial pattern of autumn crops was shaped by a dual-layer driving mechanism of "macro-geography + micro-biology" (Table 5). At the macro scale, latitude emerged as a key driver for all autumn crops, governing the broad planting zones based on the province's thermal gradient. At the micro-scale, the model used unique biological characteristics to differentiate crops: peanut was identified by its high reflectance in the red band (B4) in August, rice by its sensitivity to the Water Vapour (B9) in August, and maize and soybean by their distinct responses in the red-edge band (B5) in September.

Table 5. Top 9 most important features for crop classification based on SHAP values.

Rank	Winter Wheat	Maize	Rice	Peanut	Soybean
1	Mar B8 (NIR)	Sep B5 (Red Edge 1)	Aug B9 (Water Vapour)	Aug B4 (Red)	Sep B5 (Red Edge 1)
2	Mar B8A (NIR)	Aug B6 (Red Edge 2)	Aug B4 (Red)	Aug B9 (Water Vapour)	Aug B6 (Red Edge 2)
3	Dec 2022 NDVI	Aug B5 (Red Edge 1)	Aug LSWI	Latitude	Aug B5 (Red Edge 1)
4	Apr B12 (SWIR 2)	Aug B4 (Red)	Aug B6 (Red Edge 2)	Aug B2 (Blue)	Aug B9 (Water Vapour)
5	Apr B3 (Green)	Jul B5 (Red Edge 1)	Sep B5 (Red Edge 1)	Aug B6 (Red Edge 2)	Jul B5 (Red Edge 1)
6	Mar B7 (Red Edge 3)	Aug B9 (Water Vapour)	Aug B5 (Red Edge 1)	Aug B10 (SWIR 1)	Aug B4 (Red)
7	Jan 2023 NDVI	Latitude	Latitude	Sep B5 (Red Edge 1)	Latitude
8	Oct 2022 NDVI	Aug B2 (Blue)	Oct LSWI	Aug B5 (Red Edge 1)	Aug B10 (SWIR 1)
9	Apr B5 (Red Edge 1)	Aug B10 (SWIR 1)	Aug B2 (Blue)	Jul B5 (Red Edge 1)	Aug B2 (Blue)

This study developed a robust "seasonal monitoring" framework that outperforms traditional single-season methods through tailored feature engineering and the XGBoost algorithm. By integrating SHAP, this approach moves beyond "black-box" mapping toward "knowledge-driven" monitoring, explicitly revealing how macro-geographic and micro-biological factors drive crop distribution. While overall accuracy was high, the significant overestimation of soybean areas underscores the persistent challenge of mixed pixels in Henan's fragmented smallholder farming systems. Future work should explore sub-pixel mapping to mitigate this issue. The resulting 10-meter crop maps offer critical spatial intelligence for national food security, providing policymakers with actionable data for optimizing yield predictions, targeting insurance subsidies, and planning precision irrigation.

Acknowledgement

The authors are grateful for financial support from the Natural Science Foundation of Henan Province (242102111186, 262102211034, 262102310468) for this study.

References

Antwarg L, Miller RM, Shapira B and Rokach L 2021. Explaining anomalies detected by autoencoders using Shapley Additive Explanations. Expert. Syst. Appl. **186**: 115736.

Blickensdörfer L, Schwieder M, Pflugmacher D, Nendel C, Erasmi S and Hostert P 2022. Mapping of crop types and crop sequences with combined time series of Sentinel-1, Sentinel-2 and Landsat 8 data for Germany. Remote Sens. Environ. **269**: 112831.

Burchard-Levine V, Nieto H, Riaño D, Migliavacca M, El-Madany T, Guzinski R, Carrara A and Martín M 2021. The effect of pixel heterogeneity for remote sensing based retrievals of evapotranspiration in a semi-arid tree-grass ecosystem. Remote Sens. Environ. **260**: 20.

Cai Y, Guan K, Peng J, Wang S, Seifert C, Wardlow B and Li Z 2018. A high-performance and in-season classification system of field-level crop types using time-series Landsat data and a machine learning approach. Remote Sens. Environ. **210**: 35-47.

Chen T, and Guestrin C 2016. XGBoost: A Scalable Tree Boosting System. 22nd ACM SIGKDD International Conference on Knowledge Discovery and Data Mining (KDD), San Francisco, CA, Assoc Computing Machinery.

Diao C 2020. Remote sensing phenological monitoring framework to characterize corn and soybean physiological growing stages. Remote Sens. Environ. **248**: 18.

Dong J, Fu Y, Wang J, Tian H, Fu S, Niu Z, Han W, Zheng Y, Huang J and Yuan W 2020. Early season mapping of winter wheat in China based on Landsat and Sentinel images. Earth Syst. Sci. Data **2020**: 1-26.

Griffiths P, Nendel C and Hostert P 2019. Intra-annual reflectance composites from Sentinel-2 and Landsat for national-scale crop and land cover mapping. Remote Sens. Environ. **220**: 135-151.

Hu M, Tang H, Yu Q and Wu W 2025. A new approach for spatial optimization of crop planting structure to balance economic and environmental benefits. Sustain. Prod. Consump. **53**: 109-124.

Jin Z, Azzari G, You C, Di Tommaso S, Aston S, Burke M and Lobell DB 2019. Smallholder maize area and yield mapping at national scales with Google Earth Engine. Remote Sens. Environ. **228**: 115-128.

Maleki S, Baghdadi N, Bazzi H, Dantas C F, Ienco D, Nasrallah Y and Najem S 2024. Machine learning-based summer crops mapping using Sentinel-1 and Sentinel-2 images. Remote Sen. **16**(23): 4548.

Peng Q, Shen R, Li X, Ye T, Dong J, Fu Y and Yuan W 2023. A twenty-year dataset of high-resolution maize distribution in China. Sci. Data **10**(1): 658.

Qi H, Qian X, Shang S and Wan H 2024. Multi-year mapping of cropping systems in regions with smallholder farms from Sentinel-2 images in Google Earth Engine. Gisci. Remote Sens. **61**(1): 23.

Qiu B, Hu X, Chen C, Tang Z, Yang P, Zhu X, Yan C and Jian Z 2022. Maps of cropping patterns in China during 2015–2021. Sci. Data **9**(1): 479.

Qiu B, Huang Y, Chen C, Tang Z and Zou F 2018. Mapping spatiotemporal dynamics of maize in China from 2005 to 2017 through designing leaf moisture based indicator from Normalized Multi-band Drought Index. Comput. Electron. Agr. **153**: 82-93.

Thenkabail P and Aneece I 2019. Global hyperspectral imaging spectral-library of agricultural crops for conterminous united states v001. NASA EOSDIS Land Processes Distributed Active Archive Center (DAAC) data set: GHISACONUS. 001.

Tian X, Bai Y, Li G, Yang X, Huang J and Chen Z 2023. An adaptive feature fusion network with superpixel optimization for crop classification using Sentinel-2 imagery. Remote Sen. **15**(8): 1990.

Tufail R, Tassinari P and Torreggiani D 2025. Assessing feature extraction, selection, and classification combinations for crop mapping using Sentinel-2 time series: A case study in northern Italy. Remote Sens. Appl **38**: 101525.

Waha K, Dietrich JP, Portmann FT, Siebert S, Thornton PK, Bondeau A and Herrero M 2020. Multiple cropping systems of the world and the potential for increasing cropping intensity. Global Environ. Chang. **64**: 102131.

Wang D, Guo M, Liu S, Li Y, Dong Q, Gong X, Ge J, Wu F and Feng H 2024. Spatiotemporal evolution of winter wheat planting area and meteorology-driven effects on yield under climate change in Henan Province of China. Plants **13**(15): 2109.

Wang S, Cai T, Wen Q, Yin C, Han J and Zhang Z 2024. Spatiotemporal dynamics of ecosystem water yield services and responses to future land use scenarios in Henan Province, China. Water **16**(17): 24.

Wu B, Zhang M, Zeng H, Tian F, Potgieter AB, Qin X, Yan N, Chang S, Zhao Y and Dong Q 2023. Challenges and opportunities in remote sensing-based crop monitoring: A review. Natl. Sci. Rev. **10**(4): 290.

Xiao T, She B, Zhao J, Huang L, Ruan C and Huang W 2025. Identification of soybean planting areas using Sentinel-1/2 remote sensing data: A combined approach of reduced redundancy feature optimization and ensemble learning. Eur. J. Agron. **164**: 127480.

Yang B, Wang J, Li S and Huang X 2023. Identifying the spatio-temporal change in winter wheat–summer maize planting structure in the North China plain between 2001 and 2020. Agronomy **13**(11): 2712.

Yang S, Zhao W, Liu Y, Cherubini F, Fu B and Pereira P 2020. Prioritizing sustainable development goals and linking them to ecosystem services: A global expert's knowledge evaluation. Geogr. Sustain. **1**(4): 321–330.

You N, Dong J, Huang J, Du G, Zhang G, He Y, Yang T, Di Y and Xiao X 2021. The 10-m crop type maps in Northeast China during 2017–2019. Sci. Data **8**(1): 41.

Zhang G, Xiao X, Biradar CM, Dong J, Qin Y, Menarguez MA, Zhou Y, Zhang Y, Jin C and Wang J 2017. Spatiotemporal patterns of paddy rice croplands in China and India from 2000 to 2015. Sci. Total Environ. **579**: 82-92.

(Manuscript received on 24 September, 2025; revised on 16 March, 2026)